Journal of Applied Physics ARTICLE scitation.org/journal/jap

Mechanism of improved crystallinity by defect-modification in proton-irradiated GaAsPN photovoltaics: Experimental and first-principle calculations approach

Cite as: J. Appl. Phys. **132**, 065701 (2022); doi: 10.1063/5.0096345
Submitted: 18 April 2022 · Accepted: 11 July 2022 ·
Published Online: 8 August 2022

Keisuke Yamane,[1,a)] Yuito Maki,[1] Shun One,[1] Akihiro Wakahara,[1] Emil-Mihai Pavelescu,[2] Takeshi Ohshima,[3] Tetsuya Nakamura,[4] and Mitsuru Imaizumi[4]

AFFILIATIONS

[1]Department of Electrical and Electronic Information Engineering, Toyohashi University of Technology, 1-1 Hibarigaoka, Tempaku, Toyohashi, Aichi 441-8580, Japan
[2]National Institute for Research and Development in Microtechnologies, Hyperion University, Erou Iancu Nicolae 126 A, 077190 Voluntari, and Calea Calarasilor 169, 030615, Romania
[3]National Institutes for Quantum Science and Technology, 1233 Watanuki, Takasaki, Gunma 370-1292, Japan
[4]Japan Aerospace Exploration Agency, 2-1-1 Sengen, Tsukuba, Ibaraki 305-8505, Japan

Note: This paper is part of the Special Topic on Radiation Effects in Materials.
[a)]**Author to whom correspondence should be addressed:** yamane.keisuke.ue@tut.jp

ABSTRACT

This study presents a new model for point-defect modification in III-V-N alloys through first-principle calculations and several validation experiments conducted in our previous study, which explain the enhanced crystallinity of III-V-N alloys caused by proton irradiation and rapid thermal annealing (RTA). Validation experiments clarified that the conversion efficiency of the GaAsPN solar cell increased after proton irradiation followed by RTA, whereas that of the GaP solar cell decreased after the same process. Thus, the improved crystallinity of the GaAsPN alloy by this process is attributed to the decrease in nitrogen-related point defects in the crystal. The detailed annihilation mechanism of the nitrogen-related point defect was then studied using first-principle calculations demonstrating that the representative nitrogen-related point defects can change to a lower-energy state when a vacancy forms at its neighboring group V site, leading to the annihilation of the defects. It was concluded that vacancies created by proton irradiation enhance the annihilation of nitrogen-related point defects.

I. INTRODUCTION

Diluted nitride III-V compound alloys (III-V-N alloys) have been extensively researched owing to their unique properties caused by the significant mismatch in size and electron negativity between nitrogen and other group V atoms. One of its important properties is a large bandgap bowing owing to the introduction of a small percentage of nitrogen.[1] The bandgap of III-V-N alloys can be narrowed more than that of conventional III-V compounds while decreasing their lattice constants. Because the lattice constant is also an important parameter for crystal growth,[2] these tunable bandgaps and lattice constants provide a new methodology for fabricating light-emitting and absorption devices.[3,4]

For instance, gallium phosphide (GaP)-based III-V-N alloys, such as GaAsPN and InGaPN, can provide a wide tunable range of absorption spectra with a lattice matching condition to the silicon substrate, leading to the expectation of new materials for monolithic III-V/Si multijunction solar cells.[5,6] Previous experimental and theoretical studies have suggested the potential of III-V-N alloys for photovoltaic applications.[5–7] However, the unintentional

formation of nitrogen-induced point defects in crystals is an obstacle for practical applications.[8,9] The point defects in III-V-N alloys are mainly investigated in gallium arsenide-based diluted nitride alloys (GaAsN).[10–12] Several studies have clarified that most N atoms occupy substitutional As sites: however, a small fraction forms a variety of interstitial defects.[13]

We recently reported that the crystallinity of GaP-based III-V-N alloys can be recovered by a combination of proton and electron irradiation and rapid thermal annealing (RTA).[14] Particularly, the photoluminescence (PL) intensity of GaPN alloys and the efficiency of GaAsPN solar cells were improved compared to those of samples treated only with RTA.[14] Proton and electron beam irradiation generates point defects, most likely vacancies, in the crystal, resulting in the degradation of crystallinity.[15,16] The unique results presented in our previous study[14] suggest that these vacancies may have played a role in crystallinity enhancement.

In this study, several validation experiments with respect to our previous study are presented. Furthermore, we propose a new model for point-defect modification through first-principle calculations, which explain the enhanced crystallinity of III-V-N alloys caused by proton irradiation followed by RTA.

II. EXPERIMENTS AND CALCULATION DETAILS

A. Experiments

To clarify the effects of proton irradiation and RTA on III-V-N alloys, we prepared the following five types of solar cell samples, as shown in Table I: (a) a GaAsPN pin structure with proton irradiation followed by RTA, (b) a GaAsPN pin structure with RTA followed by proton irradiation, (c) a GaAsPN pin structure only with RTA, (d) a GaP pin structure with proton irradiation followed by RTA, and (e) a GaP pin structure only with RTA. The current density-voltage (JV) curves were characterized under AM 1.5 G and an illumination of 1 sun.

GaAsPN samples used in this study were MBE-grown pin Ga$(As_{0.2}P_{0.8})_{1-x}N_x$ (x = 0.05) solar cell structures with the estimated bandgap of 1.7 eV, identical to that used in a previous study.[14] A GaP pin solar cell structure consisting of a 100-nm-thick p^+-GaP layer ($p^+ = 1 \times 10^{19}$ cm^{-3}) and a 900-nm-thick *undoped* GaP layer on an n^+-GaP substrate was also prepared for comparison with the GaAsPN pin solar cell. Following growth, the wafers were cleaved into 12 mm × 12 mm pieces for different fabrication processes of the solar cell test devices. Proton irradiation experiments were performed for several samples [sample type (a), (b), and (d) in Table I] using a proton accelerator at the National Institute for Quantum Science and Technology. The proton fluence was set to 10^{12} cm^{-2} with an acceleration voltage of 380 keV, which is the optimum irradiation fluence revealed in a previous PL study.[14] An acceleration voltage of 380 keV was selected to enable the irradiated proton to pass through the entire epilayer. The RTA process was conducted at 920 °C for 30 s in a nitrogen ambient atmosphere before [sample type (b)] and after [sample types (a) and (d)] proton irradiation.

The GaAsPN and GaP solar cell test devices were fabricated using a standard photolithography technique. AuZn (Zn = 10%) ring electrodes and Al planar electrodes were fabricated for the GaAsPN solar cell test device as the front (p^+−GaAsPN) and back (n^+−Si) contacts, respectively. AuZn (Zn = 10%) ring electrodes and AuGe (Ge = 13%) planar electrodes were fabricated for the GaP solar cell test devices as the front (p^+-GaP) and back (n^+-GaP) contacts, respectively.

B. First-principle calculations

To clarify the atomic-scale phenomena, the first-principle approach was applied to GaPN, which is the host material of the fabricated GaAsPN solar cell. The density functional theory (DFT) base calculation was conducted for evaluating the electronic and structural properties of GaPN alloys within the Cambridge sequential total energy package (CASTEP) framework of Materials Studio.[17] We used the space group of zinc blend-type GaPN with Perdew-Brucke-Ernzerhof (PBE) exchange-correlation functional within the generalized gradient approximation (GGA).[18] An ultrasoft pseudo-potential[19] with a 517 eV cut off energy was employed for a plane-wave basis. A 2 × 2 × 2 Monkhorst and Pack k-point sampling[20] was used. The following optimized values were used as the criteria: 2×10^{-5} eV/atom, 0.05 eV/Å, 0.1 GPa, and 2×10^{-11} cm for the energy, forces, stress, and displacement, respectively.

Figure 1 presents a standard 2 × 2 × 2 GaP bulk supercell. Representative point defects deduced from the analogy of the defects in the GaAsN alloy were introduced to this supercell.[10] N_V, $(N\text{-}N)_V$, and $(N\text{-}P)_V$ indicate the substitutional single-nitrogen-atom, N-N pair, and N-P pair at group V sites, respectively. N_i and V_P denote interstitial nitrogen and phosphorus vacancies, respectively. One N_V in this supercell corresponds to a nitrogen alloy composition of 3.3%. The lattice constant of the GaP host material was fixed at 5.505 Å, which was derived using first-principle calculations, within the CASTEP framework. Note that the crystal parameters such as lattice constant and bandgap energy obtained by first-principle calculations are not always in perfect agreement with the experimental values.

TABLE I. Samples and processes employed in this study. "Proton + RTA" indicates that the sample was irradiated by a proton beam followed by RTA. "RTA + Proton" indicates that RTA was performed on the sample, followed by proton beam irradiation.

Sample type	Sample name	Structure	Proton irradiation conditions
(a)	GaAsPN proton + RTA	p^+-GaAsPN/undoped GaAsPN/GaP/n^+-Si	$V_{acc} = 380$ keV, (Fluence) = 10^{12} cm^{-2}
(b)	GaAsPN RTA + proton	p^+-GaAsPN/undoped GaAsPN/GaP/n^+-Si	$V_{acc} = 380$ keV, (Fluence) = 10^{12} cm^{-2}
(c)	GaAsPN RTA-only	p^+-GaAsPN/undoped GaAsPN/GaP/n^+-Si	No irradiation
(d)	GaP proton + RTA	p^+-GaP/undoped GaP/n^+-GaP	$V_{acc} = 380$ keV, (Fluence) = 10^{12} cm^{-2}
(e)	GaP RTA-only	p^+-GaP/undoped GaP/n^+-GaP	No irradiation

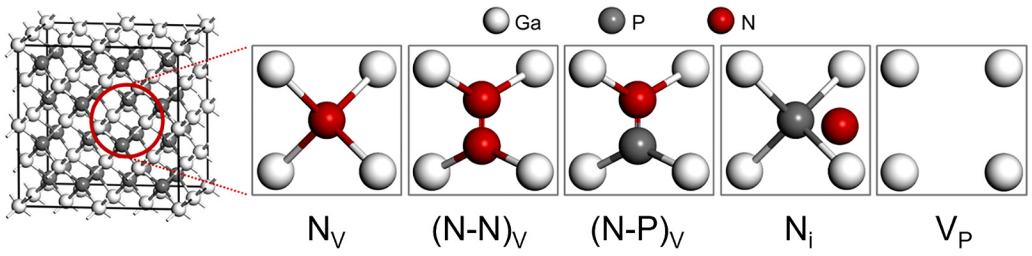

FIG. 1. The 2 × 2 × 2 supercell of GaP with representative point defects deduced from the analogy of the defects in the GaAsN alloy. N_V, $(N–N)_V$, and $(N–P)_V$ indicate the substitutional single-nitrogen-atom, N–N pair, and N–P pair at group V sites, respectively. N_i and V_P denote the nitrogen interstitial and phosphorus vacancy, respectively.

The formation energy[21] of a charge neutral defect X in GaP host is defined as follows:

$$E_{\text{form}} = E_{\text{total}}\,[\text{GaP}{:}X] - E_{\text{total}}\,[\text{GaP Bulk}] - n_X\mu_X \pm \sum n_i\mu_i$$

where E_{total} [GaP:X] is the total energy derived from a supercell calculation with one defect X in the cell and E_{total} [GaP Bulk] is the total energy for the equivalent supercell containing only bulk GaP. n_i indicates the number of atoms of type i (host atoms) added to ($n_i < 0$) or removed from ($n_i > 0$) the supercell when a defect is created and μ_i indicates the chemical potential of the species. The chemical potentials of nitrogen, phosphorus, and gallium were referenced to the N_2 molecule, P_2 molecule, and bulk gallium, respectively. To determine the possible reaction mechanism between nitrogen-related point defects and proton-induced vacancies, transition states were calculated using linear synchronous transit (LST) and quadratic synchronous transit (QST) maximization methods for the reaction pathways.[22]

III. RESULTS AND DISCUSSION

Figure 2 presents the representative JV characteristics of the GaAsPN and GaP solar cell test devices without irradiation (RTA only), when irradiated by protons followed by RTA (proton + RTA), and when RTA was followed by proton irradiation (RTA + proton). The parameters of these devices are listed in Table II. The data was collected for 10 samples of each type and almost all the data points presented a similar tendency. The conversion efficiency of the GaAsPN solar cell increased owing to proton irradiation followed by RTA, whereas that of the GaP solar cell decreased as a result of the same process. The results for both the GaAsPN and GaP samples were mainly caused by the change in J_{sc}, as shown in Fig. 2 (refer to the data of samples (a), (c), (d), and (e) in Table II). In contrast, for the GaAsPN solar cell, proton

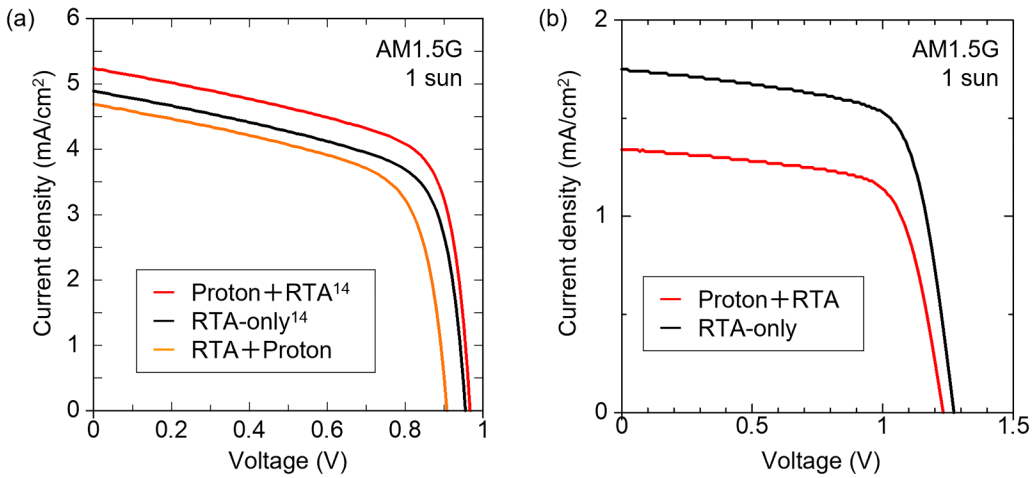

FIG. 2. Representative JV characteristics of GaAsPN and GaP solar cell test devices without irradiation (RTA only), when irradiated by protons followed by RTA (proton + RTA), and when RTA is followed by proton irradiation (RTA + proton). (a) GaAsPN solar cell and (b) GaP solar cell. Data regarding GaAsPN proton + RTA and GaAsPN RTA-only are cited from Ref. 14.

TABLE II. Parameters of the representative JV characteristics of a GaAsPN and GaP solar cell test device without irradiation (RTA only) and when irradiated by protons (proton + RTA). Data were collected under AM 1.5 G and illumination of 1 sun. J_{SC}, V_{OC}, η, and FF denote the short-circuit current density, open-circuit voltage, conversion efficiency and fill factor, respectively. Data regarding GaAsPN proton + RTA and GaAsPN RTA-only are cited from Ref. 14.

Sample type	Sample name	J_{SC} (mA/cm^2)	V_{OC} (V)	η (%)	FF (−)
(a)	GaAsPN proton + RTA[14]	5.2	0.97	3.3	0.65
(b)	GaAsPN RTA + proton	4.7	0.95	2.7	0.62
(c)	GaAsPN RTA only[14]	4.9	0.95	3.0	0.63
(d)	GaP proton + RTA	1.3	1.2	1.1	0.69
(e)	GaP RTA-only	1.8	1.3	1.5	0.69

irradiation followed by RTA improved the conversion efficiency, whereas the RTA process followed by proton irradiation was detrimental [refer to the data for samples (a), (b), and (c) in Table II]. An enhanced PL intensity promoted by proton and electron irradiation was previously reported in GaP- and GaAs-based III-V-N alloys (for example, GaPN, GaInNAs, and GaAsNBi alloys).[14,23,24] Electron irradiation was more efficient in removing non-radiative defects in GaAsN alloys than that in GaAsBi.[23] In addition, transmission electron microscopy (TEM) revealed that irradiation-induced structural defects,[25] such as hydrogen bubbles, platelets, threading dislocations, and stacking faults, were not induced in the epilayer.[14] Thus, the improved crystallinity of the GaAsPN solar cell caused by proton irradiations is attributed to the fact that the irradiated beam affected the nitrogen-related point defects.

Radiation-induced defects generated by proton irradiation are mainly caused by the displacement of gallium and phosphorus atoms, which form vacancies. Based on the results of the Stopping and Range of Ions in Matter simulation[26] of proton irradiation of the GaP material, the proton reached approximately 3 μm at the acceleration voltage employed in this study (380 keV) with repeated collisions with the host material. As a result, protons generated both gallium and phosphorus vacancies throughout the entire epilayer. Generally, the parameters of conventional solar cells, such as the short-circuit current (J_{sc}), open-circuit voltage (V_{oc}), and maximum power (P_{max}), monotonically decrease as a function of proton fluence. This tendency can be explained by the radiation degradation model proposed in a previous study.[27] However, for the GaAsPN solar cell, the parameters improved when RTA was performed after proton irradiation. The reaction and annihilation processes can be hypothesized to occur between radiation-induced vacancies and nitrogen-related point defects in GaAsPN.

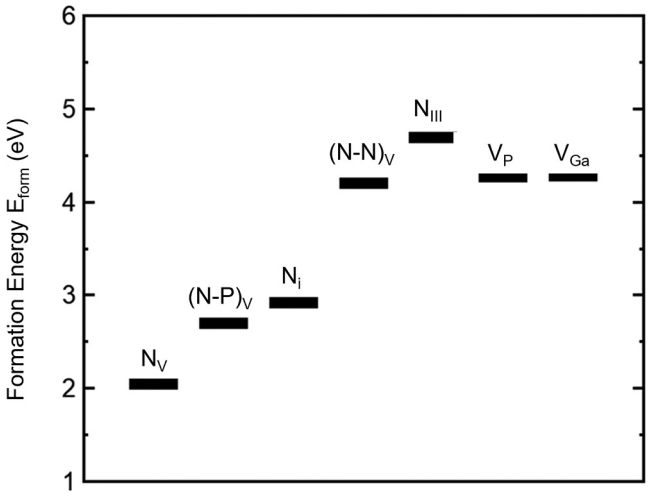

FIG. 3. Formation energy of nitrogen-related point defects. The lower formation energy indicates a more stable condition.

The formation energy of nitrogen-related point defects, which indicates their stability in the host material, was derived using first-principle calculations. Figure 3 presents the formation energy of nitrogen-related point defects. A lower formation energy indicates a more stable condition. The most stable condition for the nitrogen atoms in the GaP host was the substitutional single-nitrogen-atom at group-V sites (denoted as N_V), as shown in Fig. 1, which is consistent with GaAsN.[11] As a result, $(N\text{-}P)_V$ was the most stable nitrogen-related point defect, followed by N_i and then $(N\text{-}N)_V$.

Next, the detailed annihilation mechanisms of these defects were studied from the energy profiles of the transition of nitrogen atoms from the defect state to vacancies. Because the nitrogen antisite in the group III site (N_{III}) had a relatively large formation energy, we focused on the annihilation reaction between nitrogen-related point defects and phosphorus vacancies. Figure 4 presents the migration process of one nitrogen atom from the $(N\text{-}N)_V$ state (initial state) to the first neighboring V_P state, resulting in two N_V states (final state). The local atomic configurations and bonding states are shown in the insets. In this case, one nitrogen atom migrated above the activation energy (E_a) (0.8 eV) and reached the V_P position with a formation enthalpy (ΔH) of −3.7 eV. Thus, the $(N\text{-}N)_V$ state can change to a lower energy state when a vacancy forms at its neighboring group V site.

The transition states between representative point defects were calculated; the reaction parameters are shown in Fig. 5. The $(N\text{-}P)_V$ state with a neighboring V_P state [Fig. 5(b)] can change to the N_V state via the migration of a nitrogen atom, as in the case of $(N\text{-}N)_V$ [Fig. 5(a)]. In the case of the $(N\text{-}N)_V$ or $(N\text{-}P)_V$ state existing in the host materials without vacancies [Figs. 5(c) and 5(d)], we calculated the transition process of one nitrogen atom

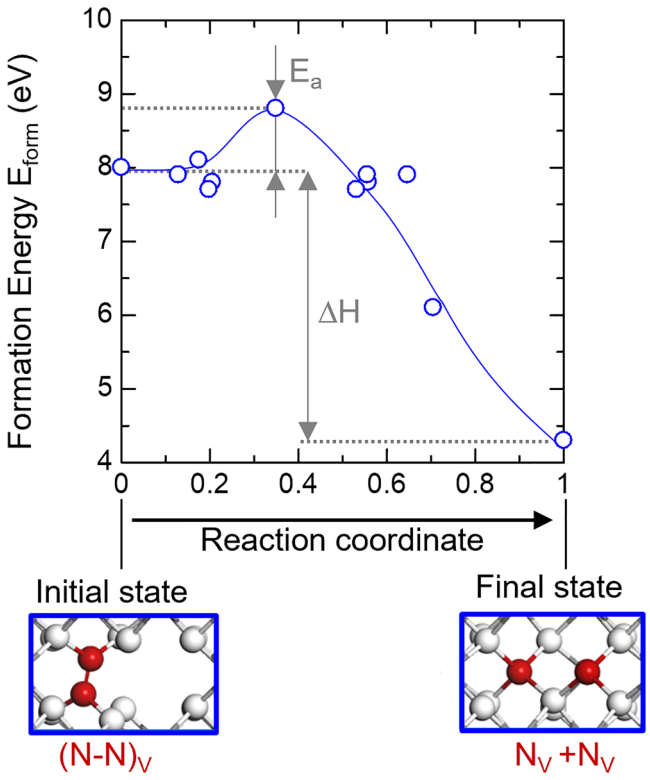

FIG. 4. Migration process of nitrogen atoms from the $(N–N)_V$ state (initial state) to the neighboring V_P state, resulting in two N_V states (final state). The local atomic configurations and bonding states are depicted in the insets. The blue line in the figure is a visual guide. Formation enthalpy (ΔH) is defined as the difference of the formation energy between the initial state and the final state of the transition process.

	Initial state		Final state		E_a (eV)	ΔH (eV)
(a)	$(N\text{-}N)_V+V_P$	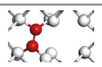	N_V+N_V	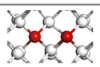	0.8	-3.7
(b)	$(N\text{-}P)_V+V_P$	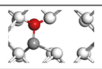	N_V	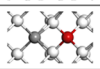	0.8	-4.6
(c)	$(N\text{-}N)_V$	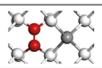	$N_V+(N\text{-}P)_V$	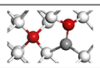	2.7	0.6
(d)	$(N\text{-}P)_V$	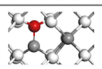	$(N\text{-}P)_V$	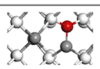	1.6	0
(e)	N_i+V_P	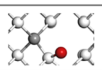	N_V	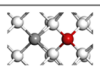	0	-5.2
(f)	N_i	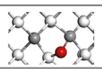	$(N\text{-}P)_V$	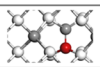	0.1	-0.2

FIG. 5. Transition states between representative point defects and their reaction parameters. The transition from the following six types of initial states are shown: (a) $(N–N)_V + V_P$, (b) $(N–P)_V + V_P$, (c) $(N–N)_V$, (d) $(N–P)_V$, (e) $N_i + V_P$, and (f) N_i.

moving to a neighboring group V site. The nitrogen atoms of the initial $(N\text{-}N)_V$ or $(N\text{-}P)_V$ states migrated over a relatively high activation energy and formed a new $(N\text{-}P)_V$ state at the neighboring position. In this case, the formation enthalpy is positive or zero, indicating an energetically unfavorable reaction. When N_i exists near the V_P [Fig. 5(e)], N_i can move to the V_P position, resulting in the N_V state. When N_i exists in the host material without any vacancies [Fig. 5(f)], N_i forms an $(N\text{-}P)_V$ state with the nearest phosphorus atom. These results led to the following speculation: despite V_P forming not only at the first neighboring group V sites of the $(N\text{-}N)_V$ position, but also at the second neighboring site, a nitrogen atom can migrate via the $(N\text{-}P)_V$ state and is finally coupled with V_P, resulting in the formation of N_V. The migration process of a nitrogen atom is likely enhanced by RTA after the irradiation process, leading to the improved crystallinity of GaAsPN materials.

IV. CONCLUSION

The wide-tunable bandgap and lattice constant of III-V-N alloys provide a new methodology for fabricating light-emitting and absorption devices. However, an obstacle for the practical application of these alloys is the unintentional formation of nitrogen-induced point defects in the crystal. This study proposes a new model for point-defect modification through validation experiments and first-principle calculations, which explains the enhanced crystallinity of III-V-N alloys caused by proton irradiation followed by RTA. The conversion efficiency of the GaAsPN solar cell increased owing to proton irradiation followed by RTA, whereas that of the GaP solar cell decreased after the same process. Thus, the improved crystallinity of the GaAsPN solar cell caused by proton irradiation is attributed to the fact that the vacancies generated by irradiation affected the nitrogen-related point defects. The detailed annihilation mechanisms of these defects were then studied from the energy profiles of the transition of nitrogen atoms from the defect state to vacancies. It was demonstrated that the representative nitrogen-related point defects can change to a lower energy state when a vacancy forms at its neighboring group V site, leading to the annihilation of the defects. It can be hypothesized that this process may be enhanced by RTA after the irradiation process, resulting in improved crystallinity of GaAsPN materials. Fabrication of GaPN solar cell test devices with and without irradiation will be a future investigation to enrich the comparison and discussion of GaAsPN and GaP solar cells.

ACKNOWLEDGMENTS

The authors gratefully acknowledge Professor Masafumi Akiyoshi (Osaka Prefecture University), Mr. Kenichi Okamoto (Osaka Prefecture University), and Mr. Mitsunobu Sugai (Advanced Engineering Services. Co., Ltd.) for their technical support in the irradiation tests. The authors thank Professor Masanobu Izaki and Professor Pei Loon Khoo (Toyohashi University of Technology) for establishing the JV measurement system. This work was financially supported by KAKENHI under a Grant-in-Aid for Scientific Research (C) 19K04488, Iwatani Foundation, Nippon Sheet Glass Foundation for Material Science and Engineering, and the Tatematsu Foundation. We would like to acknowledge Editage (www.editage.com) for the English language editing.

AUTHOR DECLARATIONS

Conflict of Interest

The authors have no conflicts to disclose.

Author Contributions

Keisuke Yamane: Conceptualization (equal); Data curation (equal); Formal analysis (equal); Funding acquisition (equal); Investigation (equal); Methodology (equal); Project administration (equal); Resources (equal); Supervision (equal); Validation (equal); Visualization (equal); Writing – original draft (equal); Writing – review and editing (equal). **Yuito Maki:** Conceptualization (equal); Data curation (equal); Formal analysis (equal); Investigation (equal); Methodology (equal); Visualization (equal). **Shun One:** Data curation (equal); Formal analysis (equal); Investigation (supporting); Methodology (supporting). **Akihiro Wakahara:** Conceptualization (equal); Funding acquisition (equal); Investigation (equal); Methodology (equal); Project administration (equal); Resources (equal); Supervision (equal). **Emil-Mihai Pavelescu:** Conceptualization (equal); Data curation (equal); Investigation (equal); Methodology (equal). **Takeshi Ohshima:** Investigation (equal); Methodology (equal); Resources (equal); Supervision (equal). **Tetsuya Nakamura:** Investigation (equal); Methodology (supporting). **Mitsuru Imaizumi:** Funding acquisition (equal); Investigation (equal); Methodology (equal); Resources (equal); Supervision (equal).

DATA AVAILABILITY

The data that support the findings of this study are available from the corresponding author upon reasonable request.

REFERENCES

[1]I. Vurgaftman and J. R. Meyer, "Band parameters for nitrogen-containing semiconductors," J. Appl. Phys. **94**(6), 3675 (2003).

[2]K. Yamane, S. Mugikura, S. Tanaka, M. Goto, H. Sekiguchi, H. Okada, and A. Wakahra, "Impact of temperature and nitrogen composition on the growth of GaAsPN alloys," J. Cryst. Growth **486**, 24–29 (2018).

[3]H. Yonezu, Y. Furukawa, and A. Wakahara, "III-V epitaxy on Si for photonics applications," J. Cryst. Growth **310**(23), 4757–4762 (2008).

[4]K. Yamane, M. Goto, K. Takahashi, K. Sato, H. Sekiguchi, H. Okada, and A. Wakahara, "Growth of a lattice-matched GaAsPN P-I-N junction on a Si substrate for monolithic III-V/Si tandem solar cells," Appl. Phys. Express **10**(7), 075504 (2017).

[5]S. Almosni, P. Rale, C. Cornet, M. Perrin, L. Lombez, A. Létoublon, K. Tavernier, C. Levallois, T. Rohel, N. Bertru, J.F. Guillemoles, and O. Durand, "Correlations between electrical and optical properties in lattice-matched GaAsPN/GaP solar cells," Sol. Energy Mater. Sol. Cells **147**, 53–60 (2016).

[6]A. Rolland, L. Pedesseau, J. Even, S. Almosni, C. Robert, C. Cornet, J. M. Jancu, J. Benhlal, O. Durand, A. Le Corre, P. Rale, L. Lombez, J.-F. Guillemoles, E. Tea, and S. Laribi, "Design of a lattice-matched III–V–N/Si photovoltaic tandem cell monolithically integrated on silicon substrate," Opt. Quantum Electron. **46**, 1397 (2014).

[7]S. Sukrittanon, R. Liu, Y. G. Ro, J. L. Pan, K. L. Jungjohann, C. W. Tu, and S. A. Dayeh, "Enhanced conversion efficiency in wide-bandgap GaNP solar cells," Appl. Phys. Lett. **107**(15), 153901 (2015).

[8]W. M. Chen, I. A. Buyanova, C. W. Tu, and H. Yonezu, "Point defects in dilute nitride III-N–As and III-N–P," Physica B **376–377**, 545–551 (2006).

[9]S. G. Spruytte, C. W. Coldren, and J. S. Harris, "Incorporation of nitrogen in nitride-arsenides: Origin of improved luminescence efficiency after anneal," J. Appl. Phys. **89**(8), 4401–4406 (2001).

[10]J. E. Lowther, S. K. Estreicher, and H. Temkin, "Nitrogen-related complexes in gallium arsenide," Appl. Phys. Lett. **79**(2), 200–202 (2001).

[11]S. B. Zhang and S.-H. Wei, "Nitrogen solubility and induced defect complexes in epitaxial GaAs:N," Phys. Rev. Lett. **86**(9), 1789–1792 (2001).

[12]E. Arola, J. Ojanen, H.-P. Komsa, and T. T. Rantala, "Atomic and electronic structures of N interstitials in GaAs," Phys. Rev. B **72**(4), 45222 (2005).

[13]W. Li, M. Pessa, and J. Likonen, "Lattice parameter in GaNAs epilayers on GaAs: Deviation from Vegard's law," Appl. Phys. Lett. **78**(19), 2864–2866 (2001).

[14]K. Yamane, R. Futamura, S. Genjo, D. Hamamoto, Y. Maki, E.-M. Pavelescu, T. Ohshima, T. Sumita, M. Imaizumi, and A. Wakahara, "Improved crystallinity of GaP-based dilute nitride alloys by proton/electron irradiation and rapid thermal annealing," Jpn. J. Appl. Phys. 61, 020907 (2022).

[15]S. Sato, H. Miyamoto, M. Imaizumi, K. Shimazaki, C. Morioka, K. Kawano, and T. Ohshima, "Degradation modeling of InGaP/GaAs/Ge triple-junction solar cells irradiated with various-energy protons," Sol. Energy Mater. Sol. Cells **93**, 768–773 (2009).

[16]Y. Okuno, N. Ishikawa, M. Akiyoshi, H. Ando, M. Harumoto, and M. Imaizumi, "Degradation prediction using displacement damage dose method for AlInGaP solar cells by changing displacement threshold energy under irradiation with low-energy electrons," Jpn. J. Appl. Phys. **59**(7), 074001 (2020).

[17]S. J. Clark, M. D. Segall, C. J. Pickard, P. J. Hasnip, M. I. J. Probert, K. Refson, and M. C. Payne, "First principles methods using CASTEP," Z. Krist. Cryst. Mater. **220**(5–6), 567–570 (2005).

[18]J. P. Perdew, J. A. Chevary, S. H. Vosko, K. A. Jackson, M. R. Pederson, D. J. Singh, and C. Fiolhais, "Atoms, molecules, solids, and surfaces: Applications of the generalized gradient approximation for exchange and correlation," Phys. Rev. B **46**(11), 6671–6687 (1992).

[19]G. B. Bachelet, D. R. Hamann, and M. Schlüter, "Pseudopotentials that work: From H to Pu," Phys. Rev. B **26**(8), 4199–4228 (1982).

[20]H. J. Monkhorst and J. D. Pack, "Special points for Brillouin-zone integrations," Phys. Rev. B **13**(12), 5188–5192 (1976).

[21]S. Zhang and J. Northrup, "Chemical potential dependence of defect formation energies in GaAs: Application to Ga self-diffusion," Phys. Rev. Lett. **67**(17), 2339–2342 (1991).

[22]S. Fischer and M. Karplus, "Conjugate peak refinement: An algorithm for finding reaction paths and accurate transition states in systems with many degrees of freedom," Chem. Phys. Lett. **194**(3), 252–261 (1992).

[23]E.-M. Pavelescu, O. Ligor, J. Occena, C. Ticoș, A. Matei, R. L. Gavrilă, K. Yamane, A. Wakahara, and R. S. Goldman, "Influence of electron irradiation and rapid thermal annealing on photoluminescence from GaAsNBi alloys," Appl. Phys. Lett. **117**(14), 142106 (2020).

[24]E.-M. Pavelescu, A. Gheorghiu, M. Dumitrescu, A. Tukiainen, T. Jouhti, T. Hakkarainen, R. Kudrawiec, J. Andrzejewski, J. Misiewicz, N. Tkachenko, V. D. S. Dhaka, H. Lemmetyinen, and M. Pessa, "Electron-irradiation enhanced photoluminescence from GaInNAs/GaAs quantum wells subject to thermal annealing," Appl. Phys. Lett. **85**(25), 6158–6160 (2004).

[25]H. J. Woo, H. W. Choi, G. D. Kim, J. K. Kim, and K. J. Kim, "Blistering/exfoliation kinetics of GaAs by hydrogen and helium implantations," Surf. Coatings Technol. **203**(17–18), 2370–2374 (2009).

[26]J. F. Ziegler, M. D. Ziegler, and J. P. Biersack, "SRIM—The stopping and range of ions in matter (2010)," Nucl. Instrum. Methods Phys. Res. B **268**(11–12), 1818–1823 (2010).

[27]M. Yamaguchi, "Radiation-resistant solar cells for space use," Sol. Energy Mater. Sol. Cells **68**(1), 31–53 (2001).